# Dynamic Modeling of a Refrigerant-Based Cross-flow Heat Exchanger for Close-Coupled Hybrid Cooled Data Centers

Carol Caceres, Alfonso Ortega, Gerard F. Jones
Department of Mechanical Engineering Villanova University, Villanova, USA
acacere4@villanova.edu

Abstract—Close-coupled hybrid cooling systems (CCHCS) are an efficient solution for cooling of modern high-density data centers (DC). Such systems are installed in proximity to the IT equipment and offer advantages over centralized DC in terms of managing hot spots and providing demand-based cooling while eliminating raised floors. By their on-demand nature, closecoupled cooling systems must operate in dynamic modes in which their capacity, controlled by mass flow rate and operating states are in response to load variations. CCHCS feature a cross-flow heat exchanger (HX) with refrigerant or chilled water as the working fluid. The present work implements a numerical model to predict the transient response of a refrigerant-based, crossflow HX as part of a CCHCS. The use of refrigerants enhances the thermal performance of these systems by taking advantage of the high heat-transfer coefficients and high latent heat absorption obtained during the boiling process. The model assumes the refrigerant enters the HX as a sub-cooled liquid, with perhaps a few to 10 degrees C of subcooling. A system of partial differential equations for conservation of mass, energy, and momentum representing each of the flow phases for the refrigerant, HX tube wall and fins, and air is solved in MATLAB. A trapping method is implemented to capture the phase change locations (i.e., a 'front tracking' method) inside the HX, including the transition from single to two-phase and v.v. The temperature of the air entering the HX is varied over time to simulate the air leaving the servers in a DC rack. The model is validated against preliminary experimental data obtained in our laboratory for chilled water flowing in single phase. Understanding and modeling the dynamic behavior of a crossflow HX will provide insight regarding the effectiveness of CCHCS systems with subcooled inlet conditions. This can augment the control strategies implemented for cooling of data centers.

Index Terms—Data center, cross-flow heat exchanger, refrigerant, two-phase flow.

# Nomenclature

Α	Area, m <sup>2</sup>
Во	Boiling number
Co	Convective number
С	Specific heat, J/kg·K
D	Diameter, m
F	Friction force, Pa/m
f	Friction factor
$F_fl$	Fluid-dependent parameter
G	Mass flux, kg/m² · s
Н	Heat transfer coefficient, W/m <sup>2</sup> · K
h	Enthalpy, J/kg·K
Р	Perimeter, m

Pr	Prandtl number
Re	Reynolds number
р	Pressure, Pa
M	Mass, kg
ṁ	Mass flow rate, kg/s
L	Length, m
k	Heat conductivity, W/m $\cdot$ K
S	Slip ratio
Т	Temperature, K
t	Time, s
u	Velocity, m/s
x	Thermodynamic quality
У	Position, m
Z	Position, m

## Greek letters

α	Void fraction
η	Fin efficiency
ρ	Density, kg/m <sup>3</sup>
μ	Dynamic viscosity, Pa · s

### Subscripts

a	Air
c- a	Cross-sectional area
go	Vapor only
1	Saturated liquid
lo	Liquid only
r	Refrigerant
V	Saturated vapor
W	Wall
Z	Coordinate in direction of the fluid flow
1φ	Single phase
2φ	Two phase

### I. INTRODUCTION

Cloud, streaming, social platforms, and computing services have increased the demands of data centers, hastening their construction around the world. At the same time, the need for cooling techniques that provide reliable environments for IT equipment has been studied. Several sophisticated cooling technologies appeared during the past few years, such as single and two-phase on-chip cold plates, but air cooling continues

to show more reliability in terms of commissioning and safe operating conditions for electronics that are present on the servers. Besides, air can provide cooling not just to CPUs and GPUs, but also the rest of the heat-generating components.

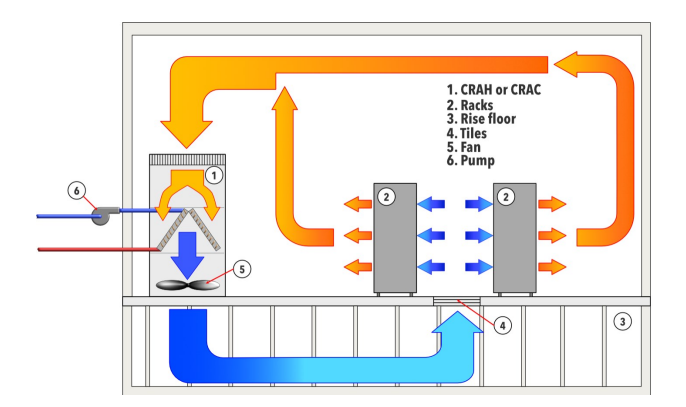


Fig. 1. Legacy Data center.

Air-cooled technologies have been extensively used in legacy data centers [1]–[5]. Cold air is supplied by CRAH or CRAC units and distributed through a raised floor and perforated tiles (see Fig. 1). This type of data center has several disadvantages, such as cooling over-provisioning, non-uniform flow distribution, problems to overcome the presence of hot spots, and mixing between cold and air streams that degrade degrading cooling capacity. Cold or hot aisle containment is used to prevent short-circuiting between the streams, but overpressure on the aisles will generate backflows.

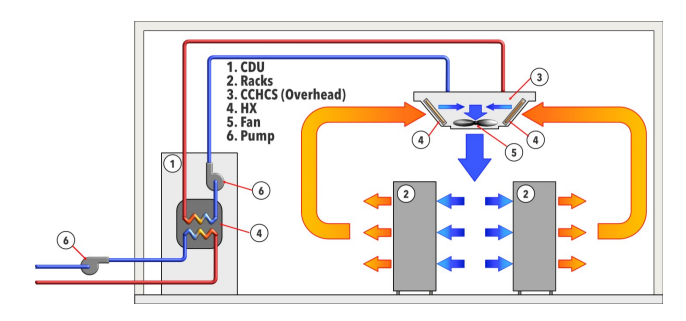


Fig. 2. Close-coupled hybrid cooling systems (CCHCS).

Since chip power density has increased, there is a concern about the air cooling limits. Air is still widely used by the industry. In order to extend air cooling capability and increase cooling efficiency, technologies such as rear doors, overhead, and in-row coolers have appeared (Fig. 2). These devices offer clear advantages compared to the legacy data center. For example, a raised floor is no longer needed. Also, the close proximity next to the IT can overcome hot spots. Another novel characteristic is that these types of systems possess an active fan that can provide cooling on demand, as the IT thermal load is variable in time. Therefore, to provide cooling as is required by the servers implies understanding the dynamic response of the CCHCS. Thus, the transient behavior of a cross-flow HX with a refrigerant as the working fluid must be predicted.

Several authors have produced single-phase models for air-to-water HXs for data centers [6]–[11]. The governing equa-

tions are complicated, nonlinear, and conjugate (i.e. more than one part of the system is modeled and the parts are coupled). Thus, the equations must be solved numerically. There are few transient studies of cross-flow HXs with refrigerants replacing chilled water for data centers. Since the refrigerant possesses a low boiling point, the two-phase physics must be considered in addition to the single-phase due to the level of subcooling at the refrigerant entrance. Transient studies in HX or evaporators considers superheating conditions at the outlet [12]–[17], which is the opposite of the HXs in CCHCS. In CCHCS the refrigerant leaves the HX with a quality to maximizes the heat extraction from the air and avoids dry out conditions at the outlet that will dramatically reduce the heat transfer coefficient of the refrigerant.

This paper proposes a numerical model to predict the transient behavior of a cross-flow HX that considers a sub-cooled single-phase condition at the inlet. Additionally, a trapping method is implemented to track where the single-phase ends at the two-phase starts when the saturated condition is reached in the refrigerant and where the refrigerant transitions from two-phase to single-phase flow.

### II. GOVERNING EQUATIONS AND DEFINITIONS

### A. Single-Phase Equations

In a cross-flow HX, the two fluid cross each other perpendicularly. As is shown in Fig. 3, an energy balance is performed for the HX refrigerant, air, and solid part of the HX.

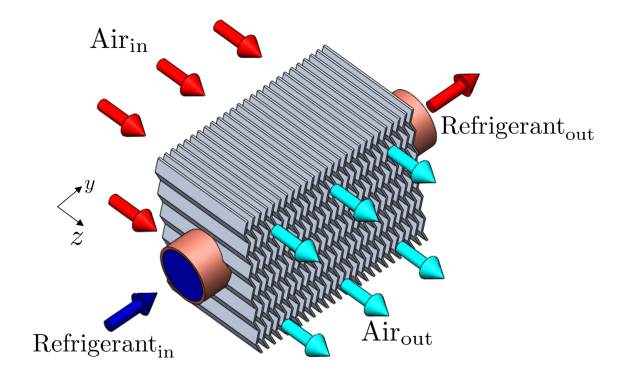


Fig. 3. Cross-flow HX representation.

We obtain,

$$M_r c_r \frac{\partial T_r}{\partial t} + \dot{m}_r c_r L_r \frac{\partial T_r}{\partial z} + H_r A_r (T_r - T_w) = 0 \quad (1)$$

$$M_a c_a \frac{\partial T_a}{\partial t} + \dot{m}_a c_a L_a \frac{\partial T_a}{\partial y} + H_a A_a \eta (T_a - T_w) = 0$$
 (2)

$$M_w c_w \frac{\partial T_w}{\partial t} + H_a A_a \eta (T_w - T_a) + H_r A_r (T_w - T_r) = 0 \quad (3)$$

Literature [18]–[21] has shown that axial conduction in the fluid and wall can be neglected for operating conditions typical of data center cooling needs and for typical HX tube-wall thickness. On the air side, the HTC (heat transfer coefficient)

was evaluated using the Wang [22] correlation. Wang proposes an extensive set of correlations for the HTC on the air side for multiple configurations and geometries. The HTC for the refrigerant working in single-phase was evaluated using the Gnielienski [23] correlation.

In this paper, we develop a front tracking method based on the thermodynamic quality defined by enthalpy, in the subcooled region where the refrigerant is liquid, and where the quality is negative (see (4)).

Equation (4) is helpful in defining the condition of the refrigerant. Thus, (4) will be a crucial expression to track the front where single-phase ends and the two-phase begins. Based on (5), a front-tracking scheme is implemented for the transition. More description about use of (5) in thermodynamics models can be found in [24] and [25].

The enthalpy h in (4) is calculated by the local absolute pressure and temperature. The saturated liquid and vapor enthalpy are obtained from local pressure and quality from (5). For single-phase, the local pressure is obtained from a momentum balance on the refrigerant. Thus,

$$\frac{\partial p}{\partial z} + F_z = 0 \tag{6}$$

The friction factor in the F<sub>z</sub> term is from Colebrook [26].

# B. Two-Phase Equations

The previous section explained how to determine the state of the refrigerant. When the saturation condition on the refrigerant side is reached, phase change begins. The energy physics in the energy equation in the refrigerant must apply to the boiling process. In previous work done by Caceres et al. [27], the authors noticed that the thermodynamic quality is found in all the equations for two-phase flow. They proposed an analysis based on Jia et al. [28]–[30], Kapadia et al. [31], and Wallis [32] to obtain an equation for thermodynamic quality. Then, from Caceres et al. [27], we obtain (7)

$$\frac{\frac{\rho_{v}}{\rho_{l}} + x \cdot 1 - \frac{\rho_{v}}{\rho_{l}}}{\frac{\rho_{v}}{\rho_{l}} + x \cdot 1 - \frac{\rho_{v}}{\rho_{l}}} \cdot \frac{\rho_{v}h_{vl}}{S} + x(x-1)\frac{dS}{dx} \cdot \frac{\partial x}{\partial t} +$$

$$Gh_{vl}\frac{\partial x}{\partial z} + \frac{\pi D}{A_{c-a}}H_r(T_r - T_w) = 0 \quad (7)$$

Equation (7) treats the for thermodynamic quality as a dependent variable of the problem. This equation considers possible slip ratio effects (for the non-homogeneous case). Slip ratio is the ratio of vapor velocity to liquid velocity. For the homogeneous approach, where the slip ratio is equal to 1, (7) becomes

$$\frac{\rho_{v} h_{vl}}{\frac{\rho_{v}}{\rho_{l}} + x \cdot 1 - \frac{\rho_{v}}{\rho_{l}}} \xrightarrow{\partial t} Gh_{vl} \xrightarrow{\partial x} \frac{dx}{dz} \xrightarrow{\pi D} H_{r}(T_{r} - T_{w}) = 0$$
(8)

For the non-homogeneous case, where the slip ratio is not 1, an empirical correlation must be used. From our inspection of the literature, two models were identified. The first, the Upper-Bound (UB), is from Spedding and Chen [33], and for the Lower-Bound (LB) Chen [34].

$$S_{\text{Sppeding}} = 2.22 \begin{array}{c} 0.35 & \rho^{1} \\ \frac{1-x}{\rho^{1}} \end{array}$$
 (9)

$$S_{Chen} = 0.18 \begin{array}{ccc} & 0.4 & 0.67 & 0.07 \\ \frac{X}{1-X} & \rho_{V} & \mu_{V} \end{array}$$
 (10)

Upon substitution of (9) and (10) into (7), the energy equation for the UB and LB slip ratios are, respectively,

$$1.443 \frac{\frac{\rho_{v}}{\rho_{l}} + x \quad 1 - \frac{\rho_{v}}{\rho_{l}}}{\frac{\rho_{v}}{\rho_{l}} + x \quad 1 - \frac{\rho_{v}}{\rho_{l}}} \frac{\rho_{v} h_{vl}}{\rho_{v} h_{vl}} \frac{\rho_{l}}{\rho_{v}} \frac{x}{1 - x} \frac{\partial x}{\partial t}$$

$$+ Gh_{fg} \frac{\partial x}{\partial z} + \frac{\pi D}{A_{c-a}} H_{r}(T_{r} - T_{w}) = 0 \quad (11)$$

$$0.108 \frac{\frac{\rho_{v}}{\rho_{l}} + x \cdot 1 - \frac{\rho_{v}}{\rho_{l}}}{\frac{\rho_{v}}{\rho_{l}} + x \cdot 1 - \frac{\rho_{v}}{\rho_{l}}} \frac{\rho_{v} h_{vl}}{\rho_{v}} \frac{0.67}{\rho_{v}} \frac{x}{1 - x} = 0.4$$

$$\frac{\frac{\rho_{v}}{\rho_{l}} + x \cdot 1 - \frac{\rho_{v}}{\rho_{l}}}{\frac{\rho_{v}}{\rho_{l}}} \frac{\partial_{v} h_{vl}}{\partial_{v}} \frac{\partial_{v} h_{vl}}{\partial_{v}} \frac{\partial_{v} h_{vl}}{\partial_{v}} \frac{\partial_{v} h_{vl}}{\partial_{v}} = 0 \quad (12)$$

H<sub>r</sub> in (8), (11), and (12), is the HTC. Inspection of the literature uncovered two different functions for HTC, which produce and UB and LB cases. For the LB, Gungor and Winterton, [35] correlation is used and is given by

$$H_{GW} = H_1 + 3000Bo^{0.86} + 0.75 = 0.41$$

$$1.12 \times \frac{V}{1-V} = \frac{\rho_V}{\rho_V} \qquad (13)$$

where,

$$H^{I} = 0.023 \frac{G(1-x)D^{0.8}}{\mu^{I}} Pr^{0.4} k_{I} \frac{1}{D}$$
 (14)

and the boiling number is defined as

Bo = 
$$\frac{q''}{Gh_{vl}} = \frac{H_r(T_w - T_r)}{Gh_{vl}}$$
 (15)

For the UB, the formulation of Kandlikar [36], which is based on which mechanism is predominant in the boiling process (nucleate or convective boiling) is adopted.

$$H_{SK} = max(H_{NBD}, H_{CBD})$$
 (16)

where,

$$H_{NBD} = 0.6683 \text{Co}^{-0.2} (1 - x)^{0.8} H_1 + 1058.0 \text{Bo}^{0.7} (1 - x)^{0.8} F_{f_1} H_1$$
 (17)

$$H_{CBD} = 1.136Co^{-0.9}(1 - x)^{0.8}H_1 + 667.2Bo^{0.7}(1 - x)^{0.8}F_{f_1}H_1$$
 (18)

and the convective number is given by,

$$Co = \frac{1 - x^{0.8}}{\rho} \rho^{1} \frac{\rho_{v}}{\rho_{v}}$$
 (19)

The refrigerant used in this study is R134a. Therefore, the fluid-dependent parameter in (17) and (18), FfI, is equal to 1.63. Additionally, the momentum equation (20) is introduced to predict the local pressure in the boiling two-phase regime. Thus,

$$\frac{\partial \tilde{p}_r u_r}{\partial t} + \frac{\gamma \tilde{p}_r u_r^2}{\partial z} = -\frac{\partial p}{\partial z} - f_z$$
 (20)

where  $\gamma$  is defined as

$$\gamma = \frac{(x - Sx - 1)(Sx - x - s)}{S}$$
 (21)

For the homogeneous case,  $\gamma$  is 1. For the non-homogeneous case, correlations (9) and (10) are introduced into (21) for each of the UB and LB slip ratios. The slip ratio will affect the average density of the refrigerant in (20), which is evaluated through void fraction definition.

In (20), the source term,  $f_z$  is the friction force due to the interaction between the vapor and the wall, and the liquid and the wall.  $f_z$  is calculated by the correlation from Muller and Heck [37] where,

$$f_z = \frac{\partial p}{\partial z} = \frac{\Delta p}{\frac{\Delta p}{\Delta z}}$$
(22)

where the pressure gradient due to two-phase is equal to that only in the liquid and corrected by the multiplier  $\varphi_{lo}$ .

$$\varphi_{to} = Y^2 x^3 + (1 - x)^{1/3} 1 + 2x(Y^2 - 1)$$
 (23)

and

$$(\Delta p/\Delta L)_{go} = \frac{(\Delta p/\Delta L)_{go}}{(\Delta p/\Delta L)_{lo}}$$
 (24)

$$\frac{\Delta p^{L}}{\Delta} = \frac{G^{2}}{2D\rho} f_{10}$$
 (25)

$$\frac{\Delta p^{L}}{\Delta} \Big|_{lo} = \frac{G^{2}}{2Dp} f_{lo}$$

$$\frac{\Delta p}{\Delta L} \Big|_{go} = \frac{G^{2}}{2D\rho_{g}} f_{go}$$
(25)

The friction factor embedded in (25) and (26) is obtained from an explicit formulation given by Fang and Zhou [38].

### III. NUMERICAL ANALYSIS

IT equipment works at variable heat loads in a data center so all cooling equipment operates in transient mode. As mentioned before, the refrigerant enters with a level of subcooling. Hence, a part of heat transfer portion happens when the refrigerant is a liquid. This is characterize by using (1), (2), (3), and (6). The two-phase phenomena are captured by (2) and (3), as well as the set of equations given by the quality expression ((8), (11), or (12)), momentum equation (20), slip ratio correlations ((9) or (10)), and heat transfer coefficient ((13) or (16)).

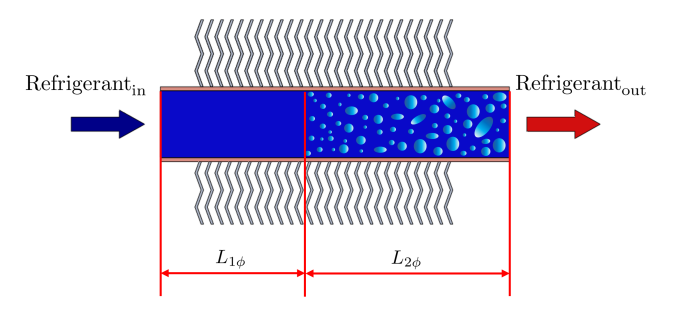


Fig. 4. Single and two-phase zones.

The finite difference method is used to solve the set of equations. A semi-implicit scheme was selected for the singlephase equations, where only the wall energy equation (3) is discretized explicitly in time. For the air (2) and refrigerant (1) energy equation, the scheme selected is upwind in space and implicit in time. As a conjugate problem, the single-phase equations are solved iteratively, where the relative convergence tolerance is 10<sup>-7</sup> based on the solution of the wall energy equation. Then, the Darcy-Weisbach equation (6) is solved for local pressure.

Two-phase equations ((8), (11), and (12)) are solved implicitly in time and upwind in space. These equations are nonlinear and are solved iteratively. In the two-phase zone as well as in the single-phase, the air (2) and wall (3) energy equations must be solved simultaneously. However, it is observed that the HTC for boiling is quality-dependent through ((8), (11), and (12)) air (2) and wall (3) equations. Therefore, in the twophase regime the HTC for the refrigerant must be updated in an iterative scheme solved for only the two-phase. Finally, the momentum equation (20) is solved for the two-phase zone.

## A. Trapping Method

Due to the level of subcooling in the refrigerant and the variable air temperature that goes into the HX, the saturated condition must be tracked. To track the phase transition, the definitions given by (4) and (5) are used. The quality value will allows us to determine where the saturated condition is reached. In other words, two zones must be characterized as is seen in Fig. 4.

In order to understand the trapping method, a graphical representation is shown in Figs. 5 and 6. When the IT load rises, the rate of boiling increase (also, the air temperature

leaving the servers increases). When this happens, the sub-cooled region shrinks and the two-phase zone increases in size (explained graphically in Fig. 5). The opposite happens when air temperature decreases. The boiling intensity is reduced and can reach the point that the refrigerant behaves only as a single-phase fluid (Fig. 6).

The numerical solution is carried out by marching in the direction of the refrigerant flow. For a fixed time, the quality is evaluated node-by-node using (4). As the quality approaches zero from a value of about  $-10^{-4}$ , we assume the next node in the direction of the refrigerant flow will be slightly positive valued. Thus, this node is identified as the transition between single-and two-phase flow. The next node downstream will possess a positive value of quality.

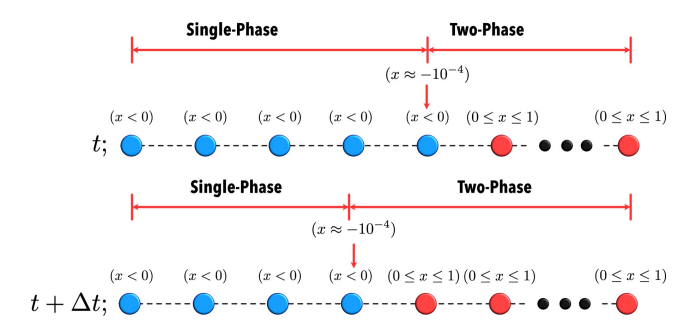


Fig. 5. Trapping method. Boiling rate increase.

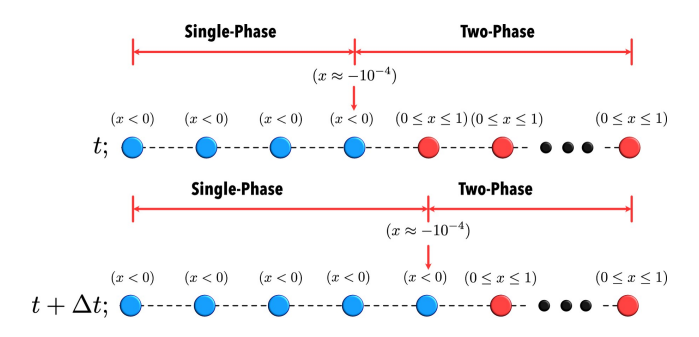


Fig. 6. Trapping method. Boiling rate decrease.

#### B. Flow Chart

The overall solution using the model proposed has multiple iterative processes. This is explained through a flow chart for single and two-phase in the calculation scheme. The number of nodes in the refrigerant direction must be high enough that at least the two first nodes are in the sub-cooled regime. The flow chart will be explained by defining a main flow chart and a different one for single and two-phase.

Figure 8 applies to the single-phase problem. Wall temperature is the criteria for convergence. After the iterative process, the local pressure is obtained. Then equation (4) is used to check if the quality is negative upon which the marching continues using single-phase equations. The flow chart shown in Fig. 9 represents all the calculation steps of the two-phase zone. Properties for the refrigerant are evaluated using REFPROP [39]. The heat transfer coefficient is a critical part of the solution process because it is embedded in nearly all of the equations in the system.

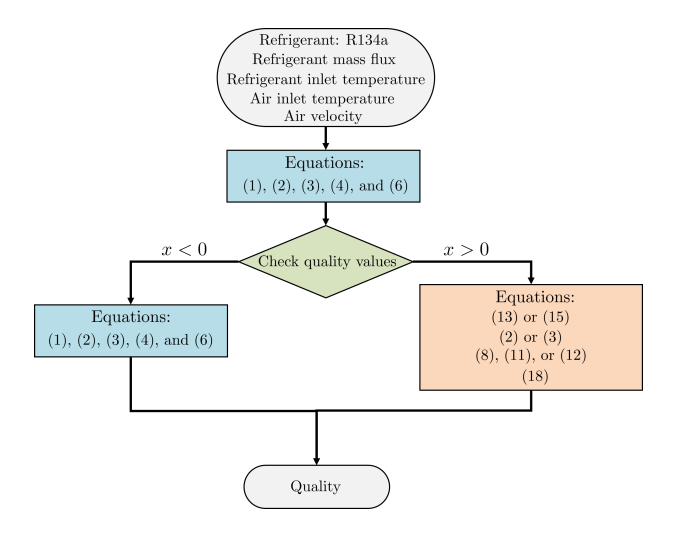


Fig. 7. Main numerical flow chart.

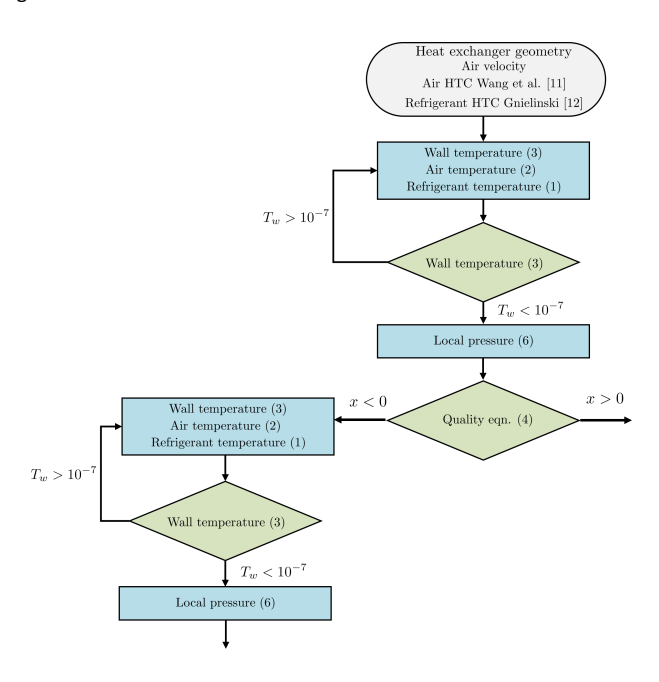


Fig. 8. Single-phase flow chart or single-phase section of the main flow chart (Fig. 7).

## C. Air Temperature Perturbation and Refrigerant Conditions

Air temperature leaving the servers in data centers changes dynamically by the computing demand. This temperature is what generates the transient behavior of the HX. To test the robustness of the code, we assumed a relatively rapid transient air temperature as seen in Fig. 10. The refrigerant inlet temperature will be set in such a way that allows a level of subcooling at the inlet. The inlet pressure will be kept constant. Pressure will generally be affected by transient behavior in the HX, but the model can dynamically consider changes in the inlet pressure. Table I shows the values used to test the numerical model.

R134a is used as the baseline because its thermodynamic properties have been well established. Is well known that green refrigerants will eventually replace R134a, therefore, the model can be adjusted to any refrigerant where properties are

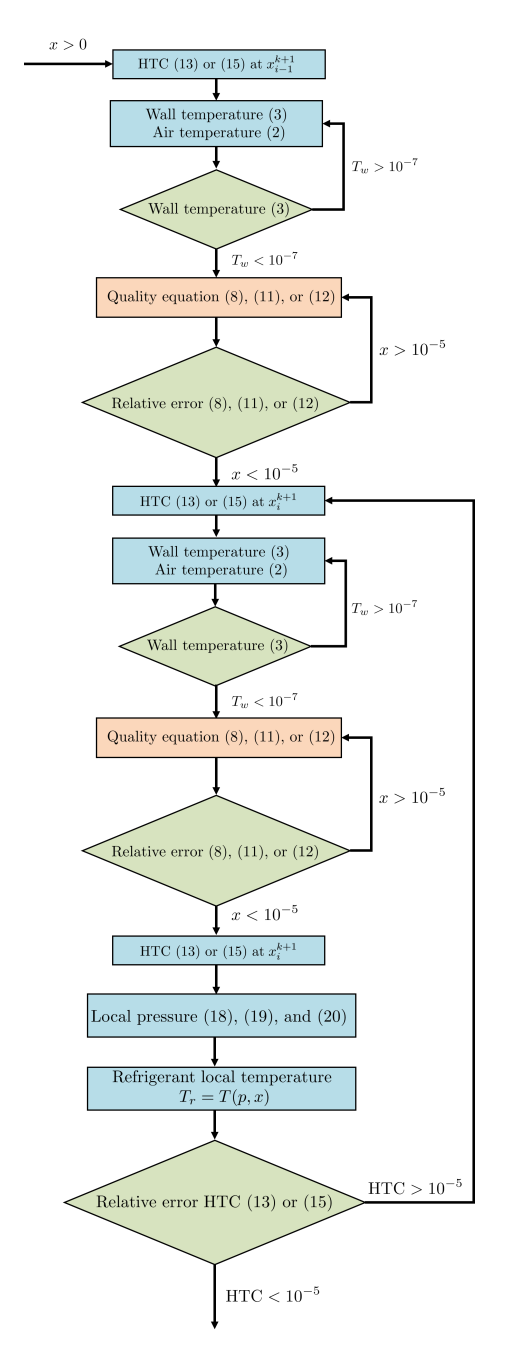


Fig. 9. Two-phase flow chart or two-phase section of the main flow chart (Fig. 7).

known and calculable.

## IV. RESULTS

Multiple cases were studied due to the high dependency on the HTC correlation and the slip ratio models chosen. Table II shows the combinations of simulations performed. A homogeneous solution is tested with two possible HTC correlations. The non-homogeneous modeling considers the cases where both slip-ratio correlations and HTCs are used in the numerical solution.

Results will focus on the quality distribution, the crucial parameter in the front tracking method developed for this work.

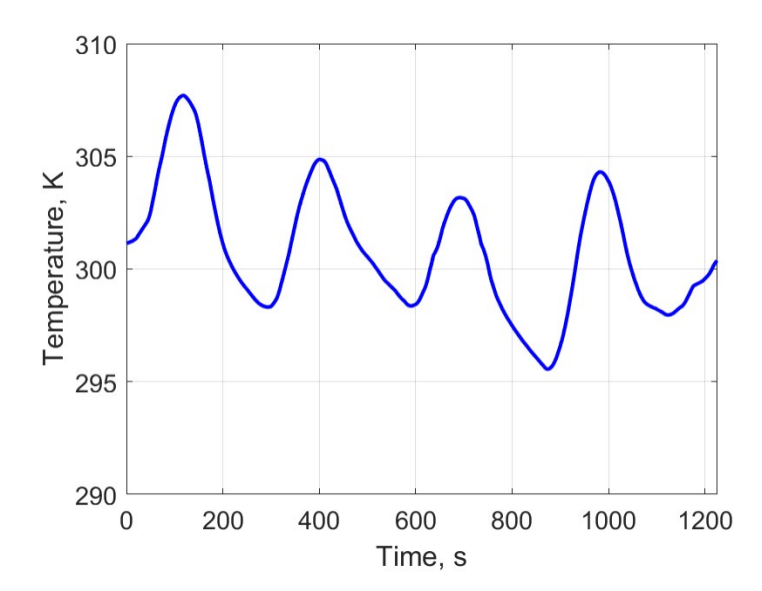


Fig. 10. Air temperature perturbation (Blue line).

TABLE I
REFRIGERANT CONDITIONS.

R134a
12°C
460 kPa
7.6°C
30 kg/m <sup>2</sup> s

### A. Homogeneous Results

The evolution of quality is presented as a function of time and distance in the direction of the flow. The non-dimensional length is defined as

$$z^{2} = \frac{z}{L}$$
 (28)

Figures 11 and 12 show how the quality changes with time and position. For the results in Fig. 11 the HTC used was the lower bound (Gungor and Winterton). The maximum quality predicted is around 20.1%.

Using the HTC for the upper limit (Kandlikar) clearly shows an effect from the higher HTC on the rate of boiling. The maximum quality produced from Fig. 12 is around 32.4%. Compared with the HTC lower bound result, the quality is about 18 percentage points larger. Hence, the HTC will have a strong influence on the boiling rate.

TABLE II CASES SIMULATED.

Model	HTC	Slip-ratio
Homogeneous (8)	Gungor and Winterton (13) [L] Kandlikar (16) [U]	-
Non-Homogeneous (11)	Gungor and Winterton (13) [L] Kandlikar (16) [U]	Spedding (9) [U]
Non-Homogeneous (12)	Gungor and Winterton (13) [L] Kandlikar (16) [U]	Chen (10) [L]

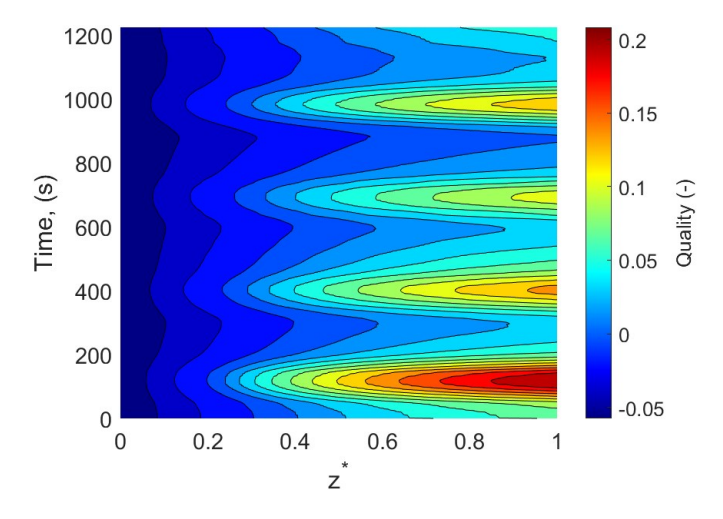


Fig. 11. Quality evolution. Homogeneous model. Gungor and Winterton HTC.

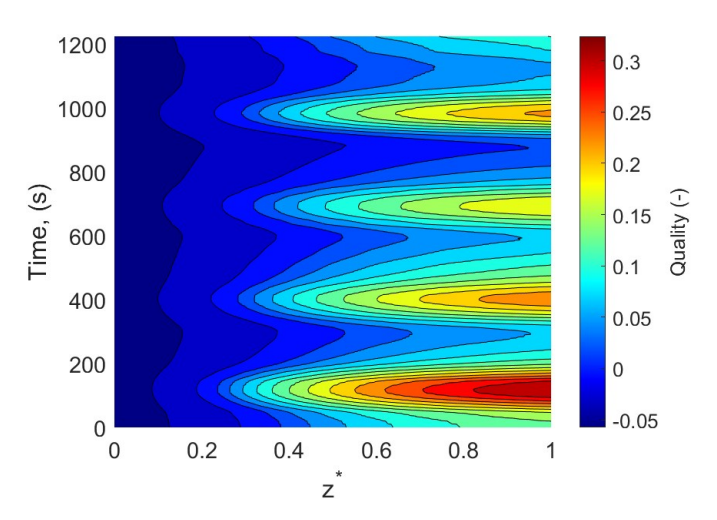


Fig. 12. Quality evolution. Homogeneous model. Kandlikar HTC.

Figure 13 shows the capability of the trapping method. The upper part of the curve corresponds to the two-phase zone. The lower portion is single-phase length due to the subcooled entrance effects. The results, which show that the single-phase region occupies nearly 40% of the tube length for much of the time, are evidence that the level of subcooling is high.

### B. Non-Homogeneous Results

Figures 14 and 15 show the slip-ratio effects for the non-homogeneous model. Comparing these results with the homogeneous case indicates a weak influence on predicted quality. This can be observed when Fig. 11 is compared with Fig. 14 or Figs. 12 and 15.

It is of interest to examine the scale of the time-dependent term in the governing equations. Figure 16 provides the behavior of the temporal term from (8), (11), and (12). From our inspection of these results, we see that for the cases examined in this paper, the scale of the coefficient of the temporal term in the energy equation at moderate quality is relatively small (of the order of 0.1). For qualities near the transition from subcooled liquid to saturation (small positive qualities), however, for at least the homogeneous case, the

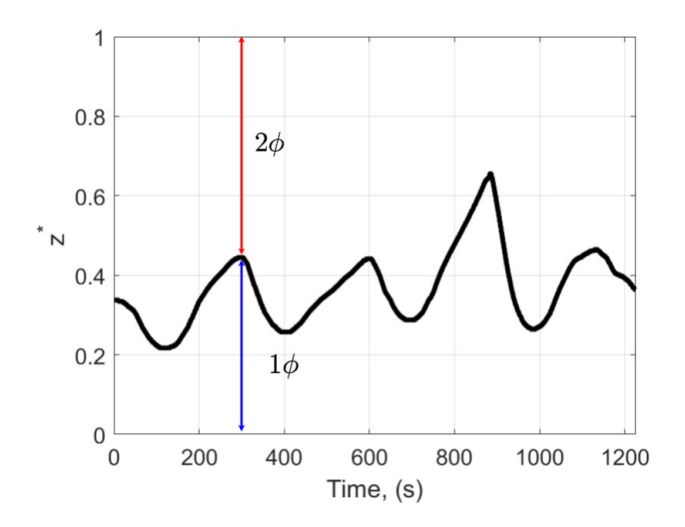


Fig. 13. Non-dimensional transitional length. Single-phase solution.

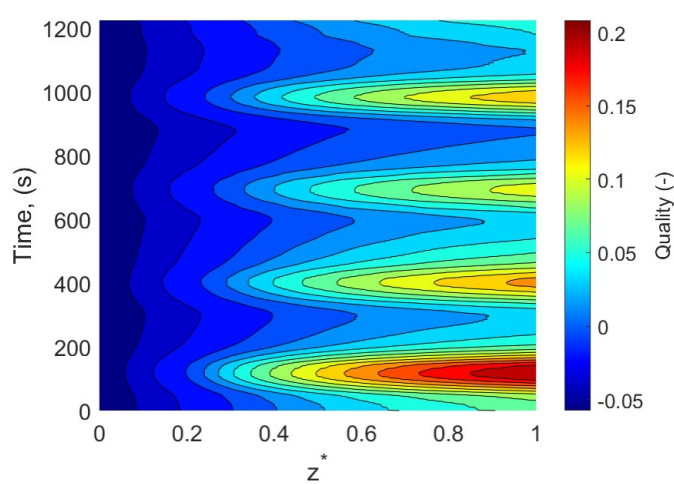


Fig. 14. Quality evolution. Non-homogeneous model [LB]. Gungor and Winterton HTC.

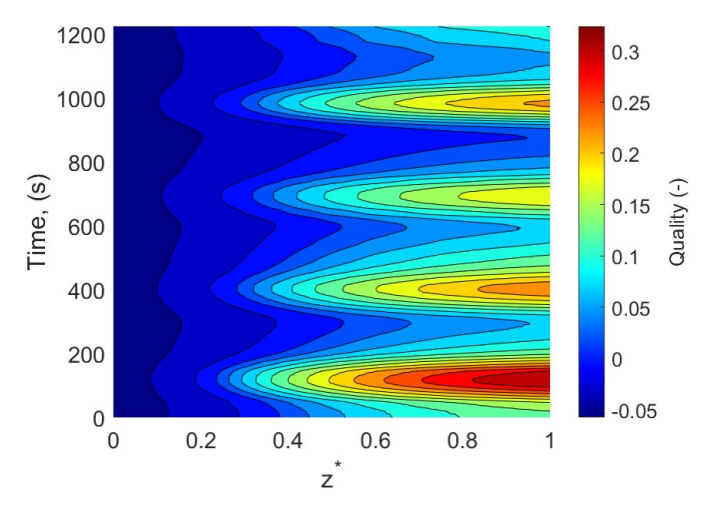


Fig. 15. Quality evolution. Non-homogeneous model [UB]. Kandlikar HTC.

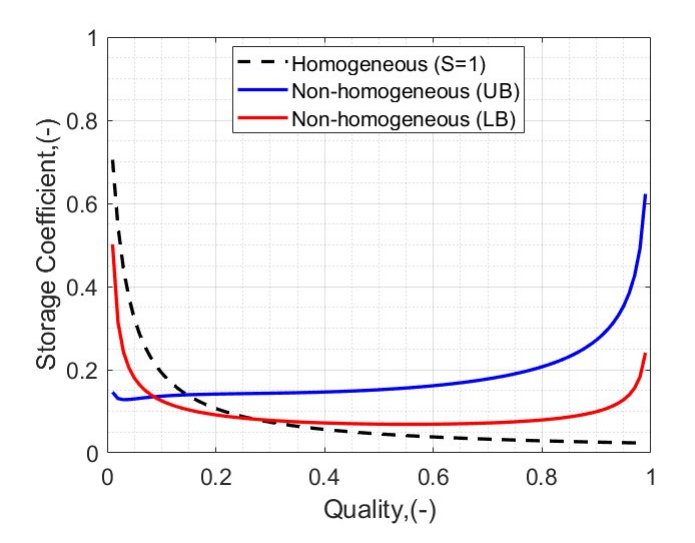


Fig. 16. Non-dimensional temporal coefficient behavior for (8), (11), and (12).

order of magnitude of this coefficient approaches 1. Thus, for cases where the quality is small and for time-dependent air temperature having higher frequencies than Fig. 10, we expect thermal performance results to be more sensitive to time shown in Figs. 11-15.

#### V. CONCLUSIONS

A complete numerical model is implemented to predict the transient two-phase behavior in cross-flow heat exchangers. The model accommodates any level of subcooling at the HX inlet.

Several results are noteworthy:

- The trapping method implemented in this work, which front-tracks the location of phase change from single-totwo-phase and v.v., appears to work well as the solution procedure was stable for nearly all cases run. The method also shows that the level of subcooling at the entrance of 7.6°C generates a substantial length where the HX performs in single-phase, not in the more thermally effective two-phase
- Slip ratio effects in the quality equation do not contribute significantly to the predictions. This is evidenced by numerical solutions and order of magnitude of the coefficient of the transient term in the energy equation
- The heat transfer coefficient correlation affects the rate of change of quality with respect to both space and time. It is noteworthy that the difference between the UB and LB HTC is just 20%. This property is highly relevant and must be carefully chosen to obtain accurate solutions for the cross-flow HX performance predictions from this

Future studies will consider experimental validation of the numerical model proposed in this work.

### ACKNOWLEDGMENT

This material is based upon the work supported by the national Science Foundation Center for Energy Smart Electronic

System (ES2) under the Grant No. IIP-1738782. Any opinions, findings, and conclusions or recommendations expressed in this material are those of the author(s) and do not necessarily reflect the views of the National Science Foundation.

#### REFERENCES

- [1] Khalaj, Ali Habibi, and Saman K. Halgamuge. "A Review on efficient thermal management of air-and liquid-cooled data centers: From chip to the cooling system." Applied energy 205 (2017): 1165-1188.
- [2] Khalaj, Ali Habibi, and Saman K. Halgamuge. "A Review on efficient thermal management of air-and liquid-cooled data centers: From chip to the cooling system." Applied energy 205 (2017): 1165-1188.
- [3] Ebrahimi, Khosrow, Gerard F. Jones, and Amy S. Fleischer. "A review of data center cooling technology, operating conditions and the corresponding low-grade waste heat recovery opportunities." Renewable and Sustainable Energy Reviews 31 (2014): 622-638.
- [4] Ahmadi, Vahid Ebrahimpour, and Hamza Salih Erden. "A parametric CFD study of computer room air handling bypass in air-cooled data centers." Applied Thermal Engineering 166 (2020): 114685.
- [5] Fulpagare, Yogesh, and Atul Bhargav. "Advances in data center thermal management." Renewable and Sustainable Energy Reviews 43 (2015): 981-996.
- [6] Del Valle, Marcelo, and Alfonso Ortega. "Numerical and compact models to predict the transient behavior of cross-flow heat exchangers in data center applications." Fourteenth Intersociety Conference on Thermal and Thermomechanical Phenomena in Electronic Systems (ITherm). IEEE, 2014.
- [7] Del Valle, Marcelo, Carol Caceres, and Alfonso Ortega. "Transient modeling and validation of chilled water based cross flow heat exchangers for local on-demand cooling in data centers." 2016 15th IEEE Intersociety Conference on Thermal and Thermomechanical Phenomena in Electronic Systems (ITherm). IEEE, 2016.
- [8] Del Valle, Marcelo, and Alfonso Ortega. "Experimental Characterization of the Transient Response of Air/Water Crossflow Heat Exchangers for Data Center Cooling Systems." International Electronic Packaging Technical Conference and Exhibition. Vol. 56888. American Society of Mechanical Engineers, 2015.
- [9] Del Valle, Marcelo, Carol Caceres, Alfonso Ortega, Kourosh Nemati, and Bahgat Sammakia. "Quasi-steady modeling of data center heat exchanger under dynamic conditions." In 2017 16th IEEE Intersociety Conference on Thermal and Thermomechanical Phenomena in Electronic Systems (ITherm), pp. 878-884. IEEE, 2017.
- [10] Gao, Tianyi, James Geer, and Bahgat Sammakia. "Nonuniform temperature boundary condition effects on data center cross flow heat exchanger dynamic performance." International Journal of Heat and Mass Transfer 79 (2014): 1048-1058.
- [11] Gao, Tianyi, Bahgat Sammakia, and James Geer. "Dynamic response and control analysis of cross flow heat exchangers under variable temperature and flow rate conditions." International Journal of Heat and Mass Transfer 81 (2015): 542-553.
- [12] Du, Yang, Tingting Liu, Yaxiong Wang, Kang Chen, Pan Zhao, Jiangfeng Wang, and Yiping Dai. "Transient behavior investigation of a regenerative dual-evaporator organic Rankine cycle with different forms of disturbances: Towards coordinated feedback control realization." Energy 235 (2021): 121437.
- [13] Li, Pengfei, Hongtao Qiao, Yaoyu Li, John E. Seem, Jon Winkler, and Xiao Li. "Recent advances in dynamic modeling of HVAC equipment. Part 1: Equipment modeling." HVAC&R Research 20, no. 1 (2014): 136-149.
- [14] Li, Pengfei, Yaoyu Li, John E. Seem, Hongtao Qiao, Xiao Li, and Jon Winkler. "Recent advances in dynamic modeling of HVAC equipment. Part 2: Modelica-based modeling." HVAC&R Research 20, no. 1 (2014): 150-161.
- [15] Afroz, Zakia, G. M. Shafiullah, Tania Urmee, and Gary Higgins. "Modeling techniques used in building HVAC control systems: A review." Renewable and sustainable energy reviews 83 (2018): 64-84.
- [16] Chernysheva, M. A., and Yu F. Maydanik. "Numerical simulation of transient heat and mass transfer in a cylindrical evaporator of a loop heat pipe." International Journal of Heat and Mass Transfer 51, no. 17-18 (2008): 4204-4215.
- [17] Joung, Wukchul, Keesool Gam, Kwangmin Park, Sungpil Ma, and Jinho Lee. "Transient responses of the flat evaporator loop heat pipe." International Journal of Heat and Mass Transfer 57, no. 1 (2013): 131-141.

- [18] Mishra, Manish, P. K. Das, and Sunil Sarangi. "Transient behavior of crossflow heat exchangers with longitudinal conduction and axial dispersion." J. Heat Transfer 126.3 (2004): 425-433.
- [19] Mishra, Manish, P. K. Das, and Sunil Sarangi. "Transient behaviour of crossflow heat exchangers due to perturbations in temperature and flow." International journal of heat and mass transfer 49.5-6 (2006): 1083-1089.
- [20] Mishra, Manish, P. K. Das, and Sunil Sarangi. "Effect of temperature and flow nonuniformity on transient behaviour of crossflow heat exchanger." International Journal of Heat and Mass Transfer 51.9-10 (2008): 2583-2592.
- [21] Syed, Fatir Hussain, and Stephen Idem. "Transient performance of a cross flow heat exchanger using finite difference analysis." ASME International Mechanical Engineering Congress and Exposition. Vol. 48715. 2008.
- [22] Wang, Chi-Chuan. "Recent progress on the air-side performance of finand-tube heat exchangers." International Journal of Heat Exchangers 1.1 (2000): 49-76.
- [23] Gnielinski, Volker. "New equations for heat and mass transfer in turbulent pipe and channel flow." Int. Chem. Eng. 16.2 (1976): 359-368
- [24] Baehr, Hans Dieter, and Karl Stephan. "Convective heat and mass transfer. Flows with phase change." Heat and Mass Transfer. Springer, Berlin, Heidelberg, 2011. 443-543.
- [25] Ghiaasiaan, S. Mostafa. Two-phase flow, boiling, and condensation: in conventional and miniature systems. Cambridge University Press, 2007.
- [26] Coolebrook, C. F. "Turbulent flow in pipes with particular reference to the transition region between the smooth and rough pipes laws." J. Inst. Civ. Eng. 11 (1939): 133-156.
- [27] Caceres, Carol, Alfonso Ortega, Aaron Wemhoff, and Gerard F. Jones. "Numerical analysis of two phase cross-flow heat exchanger for high power density equipment in data centers under dynamic conditions." In 2020 19th IEEE Intersociety Conference on Thermal and Thermomechanical Phenomena in Electronic Systems (ITherm), pp. 520-529. IEEE, 2020.
- [28] Jia, X., C. P. Tso, P. K. Chia, and P. Jolly. "A distributed model for prediction of the transient response of an evaporator." International Journal of refrigeration 18, no. 5 (1995): 336-342.
- [29] Jia, X., C. P. Tso, P. G. Jolly, and Y. W. Wong. "Distributed study of air temperature inside a dry-expansion evaporator." Applied thermal engineering 16, no. 4 (1996): 305-311.
- [30] Jia, X., C. P. Tso, P. Jolly, and Y. W. Wong. "Distributed steady and dynamic modelling of dry-expansion evaporators: Modelisation du régime stable et du régime transitoire des évaporateurs à détente sèche." International Journal of refrigeration 22, no. 2 (1999): 126-136.
- [31] Kapadia, R. G., Sanjeev Jain, and R. S. Agarwal. "Transient characteristics of split air-conditioning systems using R-22 and R-410A as refrigerants." HVAC&R Research 15, no. 3 (2009): 617-649.
- [32] Isbin, Herbert S. "One-dimensional two-phase flow, Graham B. Wallis, McGraw-Huill, New York (1969)." (1970): 896-1105.
- [33] Spedding, P. L., and J. J. J. Chen. "Correlation and estimation of holdup in two-phase flow." In Proc. NZ Geothermal Workshop, vol. 1, pp. 180-199. 1979.
- [34] Chen, J. J. "A further examination of void fraction in annular twophase flow." International journal of heat and mass transfer 29, no. 11 (1986): 1760-1763.
- [35] Gungor, K. E., and RH S. Winterton. "Simplified general correlation for saturated flow boiling and comparisons of correlations with data." Chemical engineering research & design 65, no. 2 (1987): 148-156.
- [36] Kandlikar, Satish G. "A model for correlating flow boiling heat transfer in augmented tubes and compact evaporators." (1991): 966-972.
- [37] Muller-Steinhagen, H. and, Heck, K.. "A simple friction pressure drop correlation for two-phase flow in pipes." Chemical Engineering and Processing: Process Intensification 20, no. 6 (1986): 297-308.
- [38] Fang, Xiande, Yu Xu, and Zhanru Zhou. "New correlations of single-phase friction factor for turbulent pipe flow and evaluation of existing single-phase friction factor correlations." Nuclear Engineering and Design 241, no. 3 (2011): 897-902.
- [39] Lemmon, Eric W., Ian H. Bell, M. L. Huber, and M. O. McLinden. "NIST standard reference database 23: reference fluid thermodynamic and transport properties-REFPROP, Version 10.0, National Institute of Standards and Technology." Standard Reference Data Program, Gaithersburg (2018).